

5 Point Defects in Crystals

The Russian scientist FRENKEL in 1926 [1] was the first author to introduce the concept of point defects (see Chap. 1). He suggested that thermal agitation causes transitions of atoms from their normal lattice sites into interstitial positions leaving behind lattice vacancies. This type of disorder is nowadays denoted as Frenkel disorder and contained already the concepts of vacancies and self-interstitials. Already in the early 1930s WAGNER AND SCHOTTKY [2] treated a fairly general case of disorder in binary AB compounds considering the occurrence of vacancies, self-interstitials, and of antisite defects on both sublattices.

Point defects are important for diffusion processes in crystalline solids. This statement mainly derives from two features: one is the ability of point defects to move through the crystal and to act as ‘vehicles for diffusion’ of atoms; another is their presence at thermal equilibrium. Of particular interest in this chapter are diffusion-relevant point defects, i.e. defects which are present in appreciable thermal concentrations.

In a defect-free crystal, mass and charge density have the periodicity of the lattice. The creation of a point defect disturbs this periodicity. In metals, the conduction electrons lead to an efficient electronic screening of defects. As a consequence, point defects in metals appear uncharged. In ionic crystals, the formation of a point defect, e.g., a vacancy in one sublattice disturbs the charge neutrality. Charge-preserving defect populations in ionic crystals include Frenkel disorder and Schottky disorder, both of which guarantee global charge neutrality. *Frenkel disorder* implies the formation of equal numbers of vacancies and self-interstitials in one sublattice. *Schottky disorder* consists of corresponding numbers of vacancies in the sublattices of cations and anions. For example, in AB compounds like NaCl composed of cations and anions with equal charges opposite in sign the number of vacancies in both sublattices must be equal to preserve charge neutrality. Point defects in semiconductors introduce electronic energy levels within the band gap and thus can occur in neutral or ionised states, depending on the position of the Fermi level. In what follows, we consider at first point defects in metals and then proceed to ionic crystals and semiconductors.

Nowadays, there is an enormous body of knowledge about point defects from both theoretical and experimental investigations. In this chapter, we

provide a brief survey of some features relevant for diffusion. For more comprehensive accounts of the field of point defects in crystals, we refer to the textbooks of FLYNN [3], STONEHAM [4], AGULLO-LOPEZ, CATLOW AND TOWNSEND [5], to a review on defect in metals by WOLLENBERGER [6], and to several conference proceedings [9–12]. For a compilation of data on point defects in metals, we refer to a volume edited by ULLMEIER [13]. For semiconductors, data have been assembled by SCHULZ [14], STOLWIJK [15], STOLWIJK AND BRACHT [16], and BRACHT AND STOLWIJK [17]. Properties of point defects in ionic crystals can be found in reviews by BARR AND LIDIARD [7] and FULLER [8] and in the chapters of BENIÈRE [18] and ERDELY [19] of a data collection edited by BEKE.

5.1 Pure Metals

5.1.1 Vacancies

Statistical thermodynamics is a convenient tool to deduce the concentration of lattice vacancies at thermal equilibrium. Let us consider an elemental crystal, which consists of N atoms (Fig. 5.1). We restrict the discussion to metallic elements or to noble gas solids in which the vacancies are in a single electronic state and we suppose (in this subsection) that the concentration is so low that interactions among them can be neglected. At a finite temperature, n_{1V} vacant lattice sites (monovacancies, index $1V$) are formed. The total number of lattice sites then is

$$N' = N + n_{1V}. \quad (5.1)$$

The thermodynamic reason for the occurrence of vacancies is that the Gibbs free energy of the crystal is lowered. The Gibbs free energy $G(p, T)$ of the

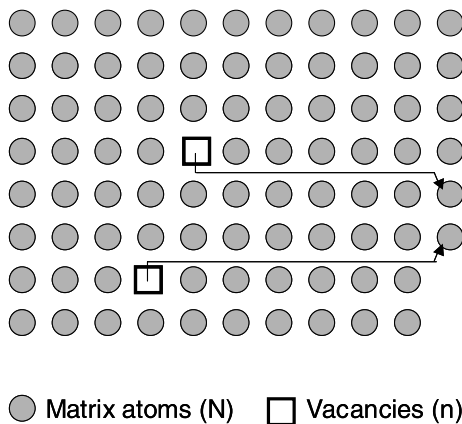


Fig. 5.1. Vacancies in an elemental crystal

crystal at temperature T and pressure p is composed of the Gibbs function of the perfect crystal, $G^0(p, T)$, plus the change in the Gibbs function on forming the actual crystal, ΔG :

$$G(p, T) = G^0(p, T) + \Delta G, \quad (5.2)$$

where

$$\Delta G = n_{1V} G_{1V}^F - T S_{\text{conf}}. \quad (5.3)$$

In Eq. (5.3) the quantity G_{1V}^F represents the *Gibbs free energy of formation* of an isolated vacancy. It corresponds to the work required to create a vacancy by removing an atom from a particular, but arbitrary, lattice site and incorporating it at a surface site ('Halbkristalllage'). Not only surfaces also grain boundaries and dislocations can act as sources or sinks for vacancies. If a vacancy is created, the crystal lattice relaxes around the vacant site and the vibrations of the crystal are also altered. The Gibbs free energy can be decomposed according to

$$G_{1V}^F = H_{1V}^F - T S_{1V}^F \quad (5.4)$$

into the *formation enthalpy* H_{1V}^F and the *formation entropy* S_{1V}^F . The last term on the right-hand side of Eq. (5.3) contains the *configurational entropy* S_{conf} , which is the thermodynamic reason for the presence of vacancies.

In the absence of interactions, all distinct configurations of n_{1V} vacancies on N' lattice sites have the same energy. The configurational entropy can be expressed through the equation of Boltzmann

$$S_{\text{conf}} = k_B \ln W_{1V}, \quad (5.5)$$

where W_{1V} is the number of distinguishable ways of distributing n_{1V} monovacancies among the N' lattice sites. Combinatoric rules tell us that

$$W_{1V} = \frac{N!}{n_{1V}! N!}. \quad (5.6)$$

The numbers appearing in Eq. (5.6) are very large. Then, the formula of Stirling, $\ln x! \approx x \ln x$, approximates the factorial terms and we get

$$\ln W_{1V} \approx (N + n_{1V}) \ln(N + n_{1V}) - n_{1V} \ln n_{1V} - N \ln N. \quad (5.7)$$

Thermodynamic equilibrium is imposed on a system at given temperature and pressure by minimising its Gibbs free energy. In the present case, this means

$$\Delta G \Rightarrow \text{Min}. \quad (5.8)$$

The equilibrium number of monovacancies, n_{1V}^{eq} , is obtained, when the Gibbs free energy in Eq. (5.3) is minimised with respect to n_{1V} , subject to the constraint that the number of atoms, N , is fixed. Inserting Eqs. (5.5) and (5.7)

into Eq. (5.3), we get from the necessary condition for thermal equilibrium, $\partial\Delta G/\partial n_{1V} = 0$:

$$H_{1V}^F - TS_{1V}^F + k_B T \ln \frac{n_{1V}^{eq}}{N + n_{1V}^{eq}} = 0 \quad (5.9)$$

By definition we introduce the *site fraction of monovacancies*¹ via:

$$C_{1V} \equiv \frac{n_{1V}}{N + n_{1V}}. \quad (5.10)$$

This quantity also represents the probability to find a vacancy on an arbitrary, but particular lattice site. In thermal equilibrium we have $C_{1V}^{eq} \equiv n_{1V}^{eq}/(N + n_{1V}^{eq})$. Solving Eq. (5.9) for the equilibrium site fraction yields

$$C_{1V}^{eq} = \exp\left(-\frac{G_{1V}^F}{k_B T}\right) = \exp\left(\frac{S_{1V}^F}{k_B}\right) \exp\left(-\frac{H_{1V}^F}{k_B T}\right). \quad (5.11)$$

This equation shows that the concentration of thermal vacancies increases via a Boltzmann factor with increasing temperature. The temperature dependence of C_{1V}^{eq} is primarily due to the formation enthalpy term in Eq. (5.11). We note that the vacancy formation enthalpy is also given by

$$H_{1V}^F = -k_B \frac{\partial \ln C_{1V}^{eq}}{\partial(1/T)}. \quad (5.12)$$

This quantity is often determined in experiments which measure relative concentrations. Such measurements are less tedious than measurements of absolute concentrations (see below). In the analysis of experiments, it is frequently assumed that formation enthalpy and entropy are independent of temperature; this is often, though not always, justified.

5.1.2 Divacancies

Divacancies (2V) are point defects that form in a crystal as the simplest complex of monovacancies (1V). This is a consequence of the mass-action equilibrium for the reaction



The probability that a given lattice site in a monoatomic crystal is vacant equals the site fraction of monovacancies. Let us suppose that a divacancy consists of two monovacancies on nearest-neighbour lattice sites. For non-interacting monovacancies, the probability of forming a divacancy is proportional to $(C_{1V})^2$. For a coordination lattice (coordination number Z) the

¹ Concentrations as number densities are given by $C_{1V}N$, when N is taken as the number density of atoms.

equilibrium fraction of divacancies C_{2V}^{eq} that form simply for statistical reasons is given by $\frac{Z}{2}(C_{1V}^{eq})^2$. However, there is also a gain in enthalpy (and entropy) when two vacancies are located on adjacent lattice sites. Fewer bonds to neighbouring atoms must be broken, when a second vacancy is formed next to an already existing one. Interactions between two vacancies are accounted for by a *Gibbs free energy of binding* G_{2V}^B , which according to

$$G_{2V}^B = H_{2V}^B - TS_{2V}^B \quad (5.14)$$

can be decomposed into an enthalpy H_{2V}^B and an entropy S_{2V}^B of interaction. For $G_{2V}^B > 0$ the interaction is attractive and binding occurs, whereas for $G_{2V}^B < 0$ it is repulsive. Combining Eq. (5.14) with the mass-action law for Eq. (5.13) yields

$$C_{2V}^{eq} = \frac{Z}{2} \exp\left(\frac{G_{2V}^B}{k_B T}\right) (C_{1V}^{eq})^2. \quad (5.15)$$

Equation (5.15) shows that at thermal equilibrium the divacancy concentration rises faster with increasing temperature than the monovacancy concentration (see Fig. 5.2). With increasing G_{2V}^B the equilibrium concentration of divacancies increases as well.

The total equilibrium concentration of vacant lattice sites, C_V^{eq} , in the presence of mono- and divacancies (neglecting higher agglomerates) is then

$$C_V^{eq} = C_{1V}^{eq} + 2C_{2V}^{eq}. \quad (5.16)$$

For a typical monovacancy site fraction in metals of 10^{-4} near the melting temperature (see below), the fraction of non-interacting divacancies would be

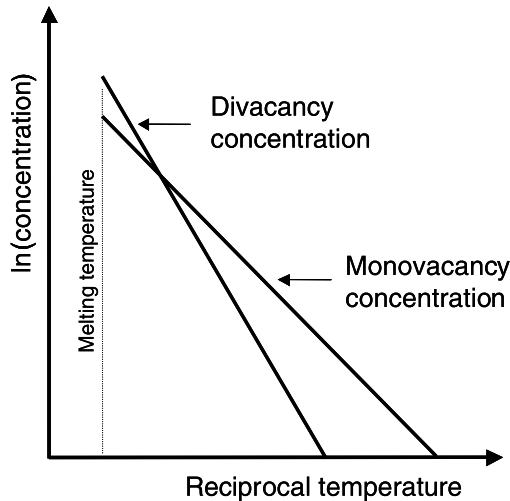


Fig. 5.2. Arrhenius diagram of equilibrium concentrations of mono- and divacancies in metals (schematic)

$\frac{Z}{2} \times 10^{-8}$. Typical interaction energies of a few 0.1 eV increase the divacancy concentration by factors of 10 to 100. Therefore, the divacancy concentration at thermal equilibrium is less or much less than that of monovacancies. Nevertheless, divacancies in close-packed metals can contribute to some extent to the diffusive transport (see Chaps. 6 and 17). The major reason is that divacancies are more effective diffusion vehicles than monovacancies, since their mobility can be considerably higher than that of monovacancies [20]. The contribution of higher agglomerates than divacancies is usually negligible.

5.1.3 Determination of Vacancy Properties

The classical method for an absolute measurement of the *total vacancy concentration*, Eq. (5.16), is **differential dilatometry (DD)**. The idea is to compare macroscopic and microscopic volume changes as functions of temperature. To understand this method, we consider a monoatomic crystal with N atoms. We denote its macroscopic volume in the defect-free state as V_0 and the volume per lattice site as Ω_0 . A defect-free state can usually be realised by cooling slowly to low enough temperatures. As long as the thermal concentration of vacant lattice sites is negligible, we have $V_0 = N\Omega_0$. With increasing temperature the volume increases due to thermal expansion and due the formation of new lattice sites. Then, the macroscopic volume and the volume per lattice site take the values $V(T)$ and $\Omega(T)$, respectively. The change in the macroscopic volume is given by

$$\Delta V \equiv V(T) - V_0 = (N + n)\Omega(T) - N\Omega_0 = N\Delta\Omega + n\Omega(T), \quad (5.17)$$

where $\Delta\Omega \equiv \Omega(T) - \Omega_0$. n is the number of new lattice sites. Equation (5.17) can be rearranged to give

$$\frac{\Delta V}{V_0} = \frac{\Delta\Omega}{\Omega_0} + \frac{n}{N} \frac{\Omega(T)}{\Omega_0}. \quad (5.18)$$

This equation reflects the two major physical reasons of the macroscopic volume change: $\Delta\Omega/\Omega_0$ is the thermal expansion of the unit cell and the second term on the right-hand side stands for the additional lattice sites.

If n_V vacant sites and n_I self-interstitials are created, we have $n = n_V - n_I$ new lattice sites. The difference between the total self-interstitial fraction, C_I^{eq} , and the total site fraction of vacant lattice sites, C_V^{eq} , is given by

$$C_V^{eq} - C_I^{eq} = \frac{\Delta V}{V_0} - \frac{\Delta\Omega}{\Omega_0}. \quad (5.19)$$

In Eq. (5.19) the effect of thermal expansion in the ratio $\Omega(T)/\Omega_0$ and higher order terms in n/N have been omitted.

In metals, self-interstitials need not to be considered as equilibrium defects (see below). We then have

$$C_V^{eq} = \frac{\Delta V}{V_0} - \frac{\Delta \Omega}{\Omega_0}. \quad (5.20)$$

For cubic crystals Eq. (5.20) can be rewritten as

$$C_V^{eq} = 3 \left(\frac{\Delta l}{l_0} - \frac{\Delta a}{a_0} \right), \quad (5.21)$$

where $\Delta l/l_0$ is the relative length change of the sample and $\Delta a/a_0$ the lattice parameter change. In deriving Eq. (5.21) from Eq. (5.20) quadratic and cubic terms in $\Delta l/l_0$ and $\Delta a/a_0$ have been neglected, because already the linear terms are of the order of a few percent or less.

Equation (5.21) shows what needs to be done in DD-experiments. The macroscopic length change and the expansion of the unit cell must be measured simultaneously². The expansion of the unit cell can be measured in very precise X-ray or neutron diffraction studies. As already mentioned, near the melting temperature of metallic elements C_V^{eq} does not exceed 10^{-3} to 10^{-4} (see Table 5.1) and is much smaller at lower temperatures. Thus, precise measurements of C_V^{eq} are very ambitious. Both length and lattice parameter changes must be recorded with the extremely high accuracy of about 10^{-6} .

Differential dilatometry experiments were introduced by FEDER AND NOWICK [21] and SIMMONS AND BALLUFFI [22, 23] around 1960 and later

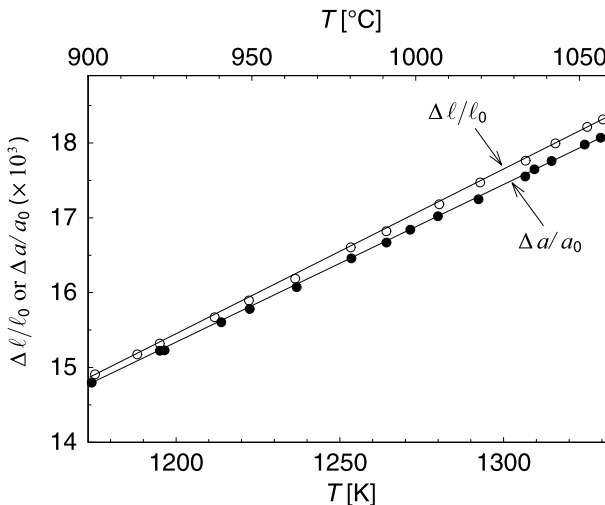


Fig. 5.3. Length and lattice parameter change *versus* temperature for Au according to SIMMONS AND BALLUFFI [23]

² For uniaxial crystals measurements in two independent directions are necessary.

used by several authors. As an example, Fig. 5.3 shows measured length and lattice parameter expansion versus temperature for gold in the interval 900 to 1060 °C according to [23]. $\Delta l/l$ is larger than $\Delta a/a$ at high temperatures due to the presence of lattice vacancies. This technique demonstrated that the dominant, thermally created defects in metals are vacancies and the exponential dependence of the vacancy concentration on temperature was also confirmed. The great advantage of DD experiments is that the total vacancy content as a function of temperature can be obtained. If monovacancies are the dominant species, both the formation enthalpy and the formation entropy can be deduced. When the divacancy contribution is not negligible, additional divacancy properties can be obtained [20].

The basic weakness of DD experiments is the insufficient accuracy in the range below about $C_V^{eq} \approx 10^{-5}$, where the divacancy contribution would be low enough to permit a direct measurement of the formation properties of monovacancies. This is illustrated for aluminium in Fig. 5.4 according to SEEGER [24]. The thermal expansion measurements of various groups [25–27] cover, with a reasonable accuracy only the concentration range between 10^{-3} to 10^{-5} . Fortunately, there are additional techniques such as positron annihilation spectroscopy (see below) that supplement DD measurements very well. An analysis of DD measurements together with these additional data yields the line in Fig. 5.4, which corresponds to a monovacancy contribution with $H_{1V}^F = 0.66$ eV and $S_{1V}^F = 0.8k_B$. Near the melting temperature the fraction of vacant sites associated as divacancies is about 50%.

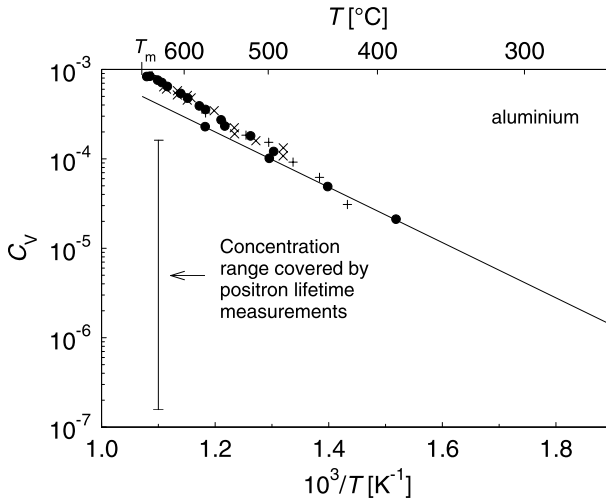


Fig. 5.4. Equilibrium concentration of vacant lattice sites in Al determined by DD measurements according to [24]. DD data: + [25], • [27], × [26]. The concentration range covered by positron lifetime measurements is also indicated

Despite the elegance of DD experiments, much information on defect properties is obtained from other ingenious experiments, which are less direct, some of which are mentioned in what follows:

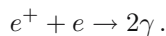
Formation enthalpies can be deduced from experiments which do not involve a determination of the absolute vacancy concentration. A frequently used method is **rapid quenching (RQ)** from high temperatures, T_Q . The quenched-in vacancy population can be studied in measurements of the residual resistivity. For example, thin metal wires or foils can be rapidly quenched. Their residual resistivities before and after quenching, ρ_0 and ρ_Q , can be measured accurately at liquid He temperature. The residual resistivity after quenching increases due to the additional scattering processes of conduction electrons at ‘frozen in’ vacancies. The increase of the residual resistivity, $\Delta\rho$, is proportional to the frozen-in vacancy concentration $C_V^{eq}(T_Q)$:

$$\Delta\rho \equiv \rho_Q - \rho_0 = \rho_V C_V^{eq}(T_Q). \quad (5.22)$$

ρ_V is a defect-related quantity, which accounts for the resistivity increase per vacant site. In a successful quenching experiment, the equilibrium vacancy population is completely ‘frozen in’. Vacancy losses to sinks such as dislocations, grain-boundaries, or surfaces can cause problems in quenching experiments. Since the residual resistivity increase per vacant site is usually unknown, only formation enthalpies can be determined from RQ experiments when $\Delta\rho$ is measured for various quenching temperatures. Formation entropies S^F are not accessible from such experiments. Only the product $\rho_V \exp(S^F/k_B)$ can be deduced.

Transmission electron microscopy (TEM) of quenched-in vacancy agglomerates is a further possibility to determine vacancy concentrations. Upon annealing vacancies become mobile and can form agglomerates. If the agglomerates are large enough they can be studied by TEM. In addition to vacancy losses during the quenching process, the invisibility of very small agglomerates can cause problems.

A very valuable tool for the determination of vacancy formation enthalpies is **positron annihilation spectroscopy (PAS)**. The positron is the antiparticle of the electron. It is, for example, formed during the β^+ decay of radioisotopes. High-energy positrons injected in metals are thermalised within picoseconds. A thermalised positron diffuses through the lattice and ends its life by annihilation with an electron. Usually, two γ -quanta are emitted according to



The energy of each γ -quantum is about 511 keV. The positron lifetime depends on the total electron density. Vacancies can trap positrons. Because of the missing core electrons at the vacant lattice site, the local electron density is significantly reduced. Therefore, the lifetime of trapped positrons is enhanced as compared to that of positrons annihilating in the perfect lattice.

Positrons in a vacancy-containing crystal end their life either by annihilation as free positrons or as trapped positrons. The lifetimes of both fates are different and the trapping probability increases with the vacancy concentration. Lifetime measurements are possible using, e.g., ^{22}Na as a positron source. This nuclide emits γ -quanta simultaneously at the ‘birth’ of the positron. The positrons ‘death’ is accompanied by the emission of two 511 keV annihilation quanta.

The interpretation of positron lifetime measurements is provided by a trapping model: a thermalised positron diffusing through a metal is trapped by a vacancy with the trapping rate σ . The positron lifetime in the trapped state, τ_t , exceeds that in the free state, τ_f , when the positron is located in an interstitial position of the perfect crystal. If untrapping is disregarded two distinct lifetimes of the positron are predicted by this model:

- (i) The trapped positron is annihilated with a lifetime τ_t .
- (ii) A positron diffusing through the crystal may end its existence as a ‘free’ particle either by the annihilation rate $1/\tau_f$ or by being trapped by a vacancy with the trapping rate σC_{1V} , where σ is the trapping cross section. This results in a lifetime given by $\tau_f/(1 + \tau_f\sigma C_{1V})$. If one assumes that initially all positrons are free, one gets for their mean lifetime:

$$\bar{\tau} = \tau_f \frac{1 + \tau_t\sigma C_{1V}}{1 + \tau_f\sigma C_{1V}}. \quad (5.23)$$

Figure 5.5 shows as an example measurements of the mean lifetime of positrons in aluminium as a function of temperature [28]. The mean lifetime increases from about 160 ps near room temperature and reaches a high

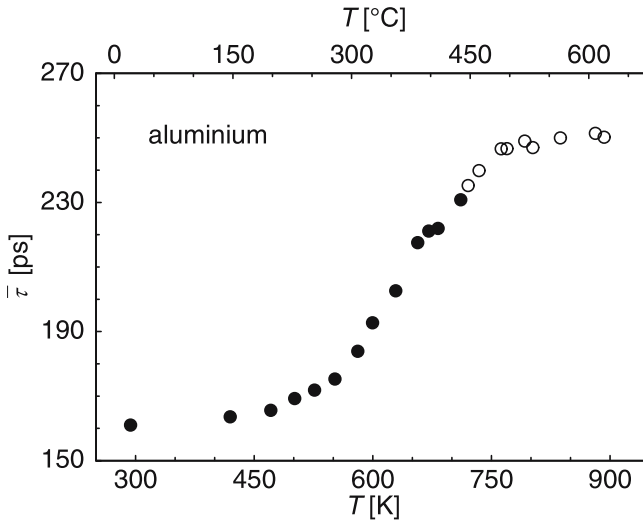


Fig. 5.5. Mean lifetime of positrons in Al according to SCHAEFER ET AL. [28]

Table 5.1. Monovacancy properties of some metals. C_{1V}^{eq} is given in site fractions

Metal	H_{1V}^F/eV	S_{1V}^F/k_B	C_{1V}^{eq} at T_m	Method(s)
Al	0.66	0.6	9.4×10^{-4}	DD + PAS
Cu	1.17	1.5	2×10^{-4}	DD + PAS
Au	0.94	1.1	7.2×10^{-4}	DD
Ag	1.09	–	1.7×10^{-4}	DD
Pb	0.49	0.7	1.7×10^{-4}	DD
Pt	1.49	1.3	–	RQ
Ni	1.7	–	–	PAS
Mo	3.0	–	–	PAS
W	4.0	2.3	1×10^{-4}	RQ + TEM

temperature value of about 250 ps. From a fit of Eq. (5.23) to the data the product σC_{1V} can be deduced. If the trapping cross section is known the vacancy concentration is accessible. If σ is constant, the vacancy formation enthalpy can be deduced from the temperature variation of σC_{1V} . At high temperature, i.e. for high vacancy concentrations, all positrons are annihilated from the trapped state. Under such conditions the method is no longer sensitive to a further increase of the vacancy concentration and the curve $\bar{\tau}$ versus T saturates. The maximum sensitivity of positron annihilation measurements occurs for vacant site fractions between about 10^{-4} and 10^{-6} (see Fig. 5.4).

A unique feature of PAS is that it is sensitive to vacancy-type defects, but insensitive to interstitials. Measurements of the mean positron lifetime is one technique of PAS. Other techniques, not described here, are measurements of the line-shape of the annihilation line and lifetime spectroscopy. Review articles on PAS applications for studies of vacancy properties in metals are provided by SEEGER [24], DOYAMA AND HASIGUTI [29], HAUTOJÄRVI [30], and SCHAEFER ET AL. [31]. Vacancy properties of metals are listed in Table 5.1 according to [6].

5.1.4 Self-Interstitials

Using statistical thermodynamics and a reasoning analogous to that for vacancies, the equilibrium fraction of self-interstitials in pure metals can be written as

$$C_I^{eq} = g_I \exp\left(-\frac{G_I^F}{k_B T}\right) = g_I \exp\left(\frac{S_I^F}{k_B}\right) \exp\left(-\frac{H_I^F}{k_B T}\right). \quad (5.24)$$

G_I^F denotes the Gibbs free energy of formation, S_I^F and H_I^F the corresponding formation entropy and enthalpy, and g_I a geometric factor. For example, in fcc metals $g_I = 3$ accounts for the fact that self-interstitials occur in the

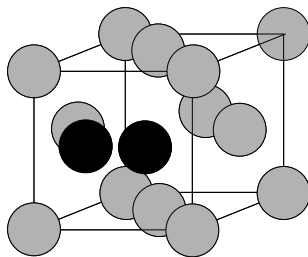


Fig. 5.6. Dumbbell configuration of a self-interstitial in an fcc lattice

so-called dumbbell configuration illustrated in Fig. 5.6, which implies three possible $\langle 100 \rangle$ orientations for a self-interstitial with its midpoint at the same lattice site.

In close-packed metals the formation enthalpy of a self-interstitial is considerably higher than that of a vacancy (see, e.g., Table 6 in the review of WOLLENBERGER [6] and the data compilation of ULLMAIER [13]):

$$H_I^F \approx (2 \text{ to } 3) \times H_{1V}^F. \quad (5.25)$$

Therefore, at thermal equilibrium

$$C_V^{eq} \gg \gg C_I^{eq}, \quad (5.26)$$

i.e. the overwhelming thermal defect population is of the vacancy type.

Self-interstitials are produced athermally (together with an equal number of vacancies), when a metal is subject to irradiation with energetic particles. Thus, self-interstitials play a significant rôle in the radiation damage and in radiation-enhanced diffusion [9, 11]. In some ionic crystals, Frenkel disorder is established at thermal equilibrium (see Sect. 5.3 and Chap. 26). For example, in silver halides Frenkel pairs are formed, which consist of self-interstitials and vacancies in the cation sublattice of the crystal.

Semiconductors are less densely packed than metals and offer more space in their interstitial sites. Therefore, the formation enthalpies of self-interstitials and vacancies are not much different. Depending on the semiconductor, both types of defects can play a rôle under thermal equilibrium conditions. This is the case for example for Si, whereas in Ge vacancies dominate self-diffusion (see Sect. 5.5 and Chap. 23).

5.2 Substitutional Binary Alloys

A knowledge of the vacancy population in substitutional alloys is of considerable interest as well. Let us consider first dilute substitutional alloys and then make a few remarks about the more complex case of concentrated alloys.

5.2.1 Vacancies in Dilute Alloys

A binary alloy of atoms B and A is denoted as dilute if the number of B atoms is not more than a few percent of the number of A atoms. Then, B is called the *solute* and A the *solvent* (or *matrix*). Depending on the solute/solvent combination interstitial and substitutional alloys are to be distinguished. Small solutes such as H, C, and N usually form interstitial alloys whereas solute atoms, which are similar in size to the solvent atoms form substitutional alloys.

In a substitutional alloy, A and B atoms and vacancies occupy sites of the same lattice. However, we have to distinguish whether a vacancy is formed on a site, where it is surrounded by A atoms only, or whether the vacancy is formed on a neighbouring site of a solute atom. In the latter case, we talk about a *solute-vacancy pair* (see Fig. 5.7). For simplicity let us suppose that the solute-vacancy interaction is restricted to nearest-neighbour sites, which is often reasonable for metals. The Gibbs free energy of vacancy formation in the undisturbed solvent, $G_{1V}^F(A)$, is different from the Gibbs free energy of vacancy formation next to a B atom, $G_{1V}^F(B)$:

$$G_{1V}^F(A) \neq G_{1V}^F(B). \quad (5.27)$$

For $G_{1V}^F(A) > G_{1V}^F(B)$ the vacancy-solute interaction is attractive, whereas for $G_{1V}^F(A) < G_{1V}^F(B)$ it is repulsive. According to LOMER [32] the total vacancy fraction in a dilute alloy, $C_V^{eq}(C_B)$, is given by

$$C_V^{eq}(C_B) = (1 - ZC_B) \exp \left[-\frac{G_{1V}^F(A)}{k_B T} \right] + ZC_B \exp \left[-\frac{G_{1V}^F(B)}{k_B T} \right], \quad (5.28)$$

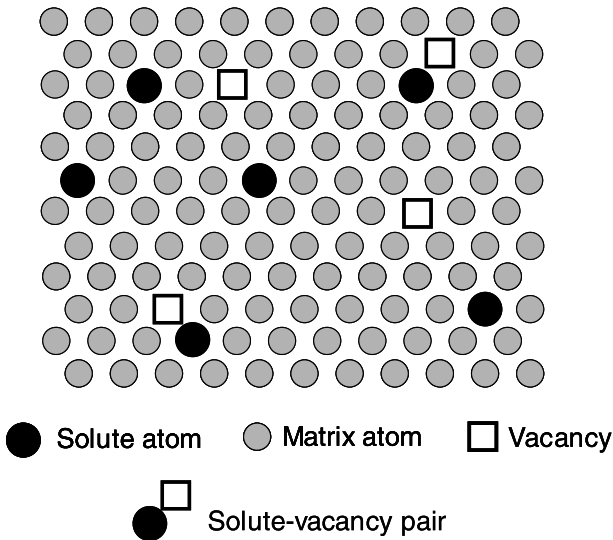


Fig. 5.7. Vacancies in a dilute substitutional alloy

where Z denotes the coordination number and C_B the solute fraction. Equation (5.28) is a good approximation for $C_B < 0.01$. We recognise that the first term corresponds to the concentration of unpaired vacancies. It is reduced by a factor $(1 - ZC_B)$ relative to that of the pure solvent. The second term is the fraction of solute-vacancy pairs. If we introduce the *Gibbs free energy of interaction* between solute and vacancy

$$G^B \equiv G_{1V}^F(A) - G_{1V}^F(B), \quad (5.29)$$

Eq. (5.28) can be written as

$$C_V^{eq} = \exp\left(-\frac{G_{1V}^F(A)}{k_B T}\right) \left[1 - ZC_B + ZC_B \exp\left(\frac{G^B}{k_B T}\right)\right] \quad (5.30)$$

and is sometimes called the *Lomer equation*.

The first factor in Eq. (5.30) is the equilibrium vacancy fraction in the pure solvent. The factor in square brackets is larger/smaller than unity if G^B is positive/negative. For binding/repulsion between solute and vacancy the total vacancy content in the alloy is higher/lower than in the pure solvent. In dilute alloys of the noble metals with solute elements lying to their right in the periodic table, G^B is typically about 0.2 eV [13]. We note that the quantity

$$p = C_{1V}^{eq} \exp\left(\frac{G^B}{k_B T}\right) \quad (5.31)$$

denotes the probability that a vacancy occupies a nearest-neighbour site of a solute, when C_{1V}^{eq} is measured in site fractions. The expressions (5.30) and (5.31) are of interest for diffusion in dilute alloys, which will be considered in Chap. 19.

5.2.2 Vacancies in Concentrated Alloys

The Lomer equation is valid for very dilute alloys ($C_B \leq 0.01$). In its derivation only associates between one solute atom and vacancy are considered. In concentrated alloys, associates between several solute atoms and vacancy and interactions between atoms of an associate become also important. To the author's knowledge robust theoretical models for the vacancy population in concentrated substitutional alloys are not available. An approximation was treated by DORN AND MITCHELL [33]. These authors attribute to each associate consisting of i solute atoms and one vacancy the (same) Gibbs free energy G_i . By standard thermodynamic reasoning, they derive the following expression for the total vacancy concentration in a concentrated alloy

$$C_V^{eq}(C_B) = \sum_{i=0}^Z \binom{Z}{i} C_A^{Z-i} C_B^i \exp\left(-\frac{G_i}{k_B T}\right), \quad (5.32)$$

where Z denotes the coordination number. The term for $i = 0$ represents the vacancy content of free vacancies in the solvent. A limitation to the terms for $i = 0$ and $i = 1$ reproduces Lomer's equation using $G_0 \equiv G_{1V}^F(A)$ and $G_i = G_{1V}^F(B)$. In the derivation of Eq. (5.32) a random distribution of atoms has been assumed. For a generalisation of Eq. (5.32) by including an interaction between atoms we refer to [34].

5.3 Ionic Compounds

Let us consider thermal defects in ionic crystals such as the alkali halides, silver chloride and bromide. These materials crystallise in sodium chloride and cesium chloride structures. They are strongly stoichiometric and have wide band gaps so that thermally produced electrons or holes can be ignored. These materials are the *classical ion conductors*, whose conductivity arises from the presence and mobility of vacancies and/or self-interstitials.

The classical ionic conductors are to be distinguished from the *fast ion conductors*. As a general rule, fast ion conductors are materials with an open structure, which allows for the rapid motion of relatively small ions. A famous example is silver iodide, for which fast ionic conduction was reported as early as 1914 [35]. It displays a first order phase transition between a fast ion-conducting phase (α -AgI) above 147°C and a normal conducting phase at lower temperatures. α -AgI has a body-centered cubic sublattice of practically immobile I^- ions. Each unit cell displays 42 interstitial sites (6 octahedral, 12 tetrahedral, 24 trigonal) over which the two Ag^+ ions per unit cell are distributed (see Fig. 27.2). Since there are many more sites than Ag^+ ions, the latter can migrate easily. Other examples are β -alumina, some compounds with fluorite structure such as some halides such as CaF_2 and PbF_2 and oxides like doped ZrO_2 , which are fluorine or oxygen ion conductors at elevated temperatures. These materials require a different approach, because in the sublattice of one ionic species the fraction of vacant sites is high (see Chap. 27).

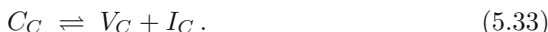
To be specific, we consider here classical ionic crystals with CA stoichiometry (C=cation, A=anion). They are composed of anions and cations which carry equal charges opposite in sign. Let us further assume that all cation sites are equivalent and all anion sites likewise; in other words, there are two filled sublattices. The defect population that can develop in such a crystal has the structural constraint that the number of C atoms and of A atoms must be equal. This can also be viewed as a condition of electroneutrality by assigning ionic charges to the atoms C and A.³ Then, only charge-preserving

³ Electroneutrality must be fulfilled in the volume of ionic crystal. In the vicinity of charged dislocations, grain boundaries or surfaces, unbalanced point defect populations can develop. In compounds with additional electronic defects the requirements of structure and of electroneutrality are different (see, e.g., the textbook of MAIER [36]).

defect populations can develop. In addition, the formation of antisite defects need not to be considered due to the high Coulomb energy of an ion placed in the ‘wrong’ sublattice. In what follows, we consider two important cases of disorder in CA ionic crystals. For a more general treatment the reader is referred, e.g., to the textbook of ALLNATT AND LIDIARD [37].

5.3.1 Frenkel Disorder

Let us suppose that vacancies (V_C) and self-interstitials (I_C) in the C sublattice are formed from cations on cation sites (C_C) according to the quasi-chemical reaction



This type of disorder is called *Frenkel disorder* (Fig. 5.8), as it was first suggested by the Russian scientist FRENKEL [1]. Pairs of vacancies and self-interstitials are denoted as Frenkel pairs. According to the law of mass action we may write

$$C_{V_C}^{eq} C_{I_C}^{eq} = \exp\left(\frac{S_{FP}}{k_B}\right) \exp\left(-\frac{H_{FP}}{k_B T}\right) \equiv K_{FP}. \quad (5.34)$$

Here $C_{V_C}^{eq}$ and $C_{I_C}^{eq}$ denote equilibrium site fractions of vacancies and self-interstitials in the C sublattice. K_{FP} is called the *Frenkel product*. The formation enthalpy H_{FP} and entropy S_{FP} for (non-interacting) Frenkel pairs can be split according to

$$H_{FP} = H_{V_C}^F + H_{I_C}^F \quad \text{and} \quad S_{FP} = S_{V_C}^F + S_{I_C}^F \quad (5.35)$$

into sums of formation enthalpies, $H_{V_C}^F + H_{I_C}^F$, and formation entropies, $S_{V_C}^F + S_{I_C}^F$, of vacancies and self-interstitials. Charge neutrality of undoped

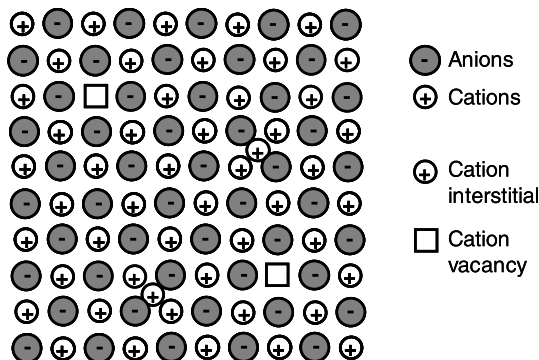


Fig. 5.8. Frenkel disorder in the cation sublattice of a CA ionic crystal

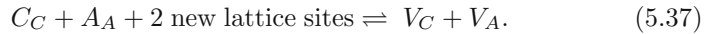
crystals requires that the numbers of vacancies and self-interstitials are equal, i.e. $C_{V_C}^{eq} = C_{I_C}^{eq}$. Then we get

$$C_{V_C}^{eq} = C_{I_C}^{eq} = \exp\left(\frac{S_{FP}}{2k_B}\right) \exp\left(-\frac{H_{FP}}{2k_B T}\right). \quad (5.36)$$

Frenkel disorder occurs in the silver sublattices of silver chloride and bromide [38, 39]. Frenkel-pair formation properties of these silver halides are listed in Table 5.2.

5.3.2 Schottky Disorder

Let us consider once more a binary ionic CA compound composed of cations on the C sublattice, C_C , and anions on the A sublattice, A_A . The constraint of electroneutrality is fulfilled, when vacancies in both sublattices, V_C and V_A , are formed according to the reaction



in equal numbers (Fig. 5.9). Applying the law of mass-action to this reaction, we get for thermal equilibrium

$$C_{V_C}^{eq} C_{V_A}^{eq} = \exp\left(\frac{S_{SP}}{k_B}\right) \exp\left(-\frac{H_{SP}}{k_B T}\right) \equiv K_{SP}, \quad (5.38)$$

where C_{V_C} and C_{V_A} denote site fractions of cation and anion vacancies, respectively. H_{SP} and S_{SP} denote enthalpy and entropy for the formation of a *Schottky pair* (cation vacancy plus anion vacancy).

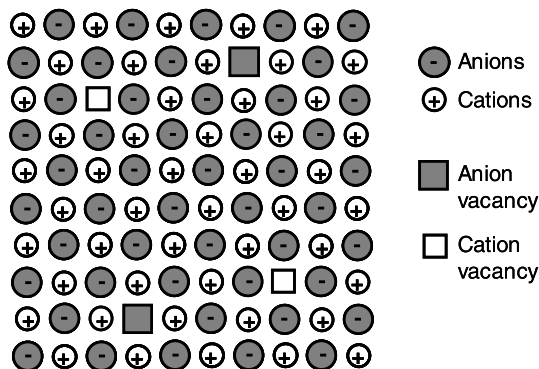


Fig. 5.9. Schottky disorder in an CA ionic crystal

Table 5.2. Formation enthalpies of Schottky- and Frenkel pairs of ionic crystals

Ionic compound	$(H_{\text{SP}} \text{ or } H_{\text{FP}})/\text{eV}$	$(S_{\text{SP}} \text{ or } S_{\text{FP}})/k_{\text{B}}$	Type of disorder
NaCl	2.44	9.8	Schottky
KCl	2.54	7.6	Schottky
NaI	2.00	7.6	Schottky
KBr	2.53	10.3	Schottky
LiF	2.68		Schottky
LiCl	2.12		Schottky
LiBr	1.80		Schottky
LiI	1.34		Schottky
AgCl	1.45–1.55	5.4–12.2	Frenkel
AgBr	1.13–1.28	6.6–12.2	Frenkel

This type of disorder is called *Schottky disorder* and K_{SP} is denoted as the *Schottky product*. Charge neutrality in an undoped crystal requires equal concentrations of cation and anion vacancies:

$$C_{\text{VC}}^{\text{eq}} = C_{\text{VA}}^{\text{eq}} = \exp\left(\frac{S_{\text{SP}}}{2k_{\text{B}}}\right) \exp\left(-\frac{H_{\text{SP}}}{2k_{\text{B}}T}\right). \quad (5.39)$$

For non-interacting Schottky pairs, the enthalpy and entropy of pair formation according to

$$H_{\text{SP}} = H_{\text{VC}}^{\text{F}} + H_{\text{VA}}^{\text{F}} \quad \text{and} \quad S_{\text{SP}} = S_{\text{VC}}^{\text{F}} + S_{\text{VA}}^{\text{F}} \quad (5.40)$$

can be expressed in terms of the formation enthalpies, H_{VC}^{F} and H_{VA}^{F} , and entropies, S_{VC}^{F} and S_{VA}^{F} , of cation and anion vacancies. Experience shows that Schottky disorder dominates the defect population in most alkali halides and in many oxides. Schottky-pair formation properties are listed in Table 5.2. Crystals doped with aliovalent ions are considered in detail in Chap. 26. In doped crystals, the Schottky product is still valid.

5.4 Intermetallics

Intermetallics are a fascinating group of materials, which attract attention from the viewpoints of fundamentals as well as applications [40, 41]. Binary intermetallics are composed of two metals or of a metal and a semimetal. Their crystal structures are different from those of the elements. This definition includes both intermetallic phases and ordered alloys. Intermetallics form a numerous and manifold group of materials and comprise a greater variety of crystal structures than metallic elements [48]. They crystallise in structures with ordered atomic distributions in which atoms are preferentially surrounded by unlike atoms. Some frequent structures are illustrated

in Chap. 20. Some intermetallics are ordered up to their melting temperature, others undergo order-disorder transitions in which an almost random arrangement of atoms is favoured at high temperatures. Such transitions occur, for example, between the β' and β phases of the Cu–Zn system or in Fe–Co. There are intermetallic phases with wide phase fields and others which exist as stoichiometric compounds. Examples for both types can even be found in the same binary alloy system. For example, the Laves phase in the Co–Nb system (approximate composition Co_2Nb) exists over a composition range of about 5 at.%, whereas the phase Co_7Nb_2 is a line compound. Some intermetallics occur for certain stoichiometric compositions only. Others are observed for off-stoichiometric compositions. Some phases compensate off-stoichiometry by vacancies, others by antisite atoms.

Thermal defect populations in intermetallics can be rather complex and we shall confine ourselves to a few remarks. Intermetallic compounds are physically very different from the ionic compounds considered in the previous section. Combination of various types of disorder are conceivable: vacancies and/or antisite defects on both sublattices can form in some intermetallics. As self-interstitials play no rôle in thermal equilibrium for pure metals, it is reasonable to assume that this holds true also for intermetallics.

To be specific, let us suppose a formula A_xB_y for the stoichiometric compound and that there is a single A sublattice and a single B sublattice. This is, for example, the case in intermetallics with the B2 and L1_2 structure (see Fig. 20.1). The basic structural elements of disorder are listed in Table 5.3.

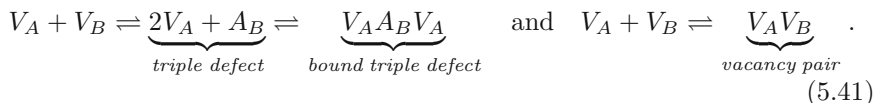
A first theoretical model for thermal disorder in a binary AB intermetallic with two sublattices was treated in the pioneering work of WAGNER AND SCHOTTKY [2]. Some of the more recent work on defect properties of intermetallic compounds has been reviewed by CHANG AND NEUMANN [42] and BAKKER [43].

In some binary AB intermetallics so-called *triple defect disorder* occurs. These intermetallics form V_A defects on the A sublattice on the B rich side and A_B antisites on the B sublattice on the A rich side of the stoichiometric composition. This is, for example, the case for some intermetallics with B2 structure where $A = \text{Ni, Co, Pd} \dots$ and $B = \text{Al, In,} \dots$ Some other intermetallics also with B2 structure such as CuZn, AgCd, \dots can maintain high concentrations of vacancies on both sublattices.

Table 5.3. Elements of disorder in intermetallic compounds

A_A	=	A atom on A sublattice
B_B	=	B atom on B sublattice
V_A	=	vacancy on A sublattice
V_B	=	vacancy on B sublattice
B_A	=	B antisite on A sublattice
A_B	=	A antisite on B sublattice

Triple defects ($2V_A + A_B$), *bound triple defects* ($V_A A_B V_A$) and *vacancy pairs* ($V_A V_B$) have been suggested by STOLWIJK ET AL. [46]. They can form according to the reactions



Very likely bound agglomerates are important in intermetallics for thermal disorder and diffusion in addition to single vacancies. In this context it is interesting to note that neither triple defects nor vacancy pairs disturb the stoichiometry of the compound.

The physical understanding of the defect structure of intermetallics is still less complete compared with metallic elements. However, considerable progress has been achieved. Differential dilatometry (DD) and positron annihilation studies (PAS) performed on intermetallics of the Fe-Al, Ni-Al and Fe-Si systems have demonstrated that the total content of vacancy-type defects can be one to two orders of magnitude higher than in pure metals [44, 45]. The defect content depends strongly on composition and its temperature dependence can show deviations from simple Arrhenius behaviour. According to SCHAEFER ET AL. [44] and HEHENKAMP [45] typical defect concentrations in these compounds near the solidus temperature can be as high as several percent.

5.5 Semiconductors

Covalent crystals such as diamond, Si, and Ge are more different from the defect point of view as one might expect from their chemical classification as group IV elements. Diamond is an electrical insulator, whose vacancies are mobile at high temperatures only. Si is a semiconductor which supports vacancies and self-interstitials as intrinsic defects. By contrast, Ge is a semiconductor in which vacancies as intrinsic defects predominate like in the metallic group IV elements Sn and Pb.

Because Si and Ge crystallise in the diamond structure with coordination number 4, the packing density is considerably lower than in metals. This holds true also for compound semiconductors. Most compound semiconductors formed by group III and group V elements like GaAs crystallise in the zinc blende structure, which is closely related to the diamond structure. Semiconductor crystals offer more space for self-interstitials than close-packed metal structures. Formation enthalpies of vacancies and self-interstitials in semiconductors are comparable. In Si, both self-interstitials and vacancies are present in thermal equilibrium and are important for self- and solute diffusion. In Ge, vacancies dominate in thermal equilibrium and appear to be the only diffusion-relevant defects (see Chap. 23 and [47, 50]).

Semiconductors have in common that the thermal defect concentrations are orders of magnitude lower than in metals or ionic crystals. This is a consequence of the covalent bonding of semiconductors. Defect formation energies in semiconductors are higher than in metals with comparable melting temperatures. Neither thermal expansion measurements nor positron annihilation studies have sufficient accuracy to detect the very low thermal defect concentrations.

Point defects in semiconductors can be neutral and can occur in various electronic states. This is because point defects introduce energy levels into the band gap of a semiconductor. Whether a defect is neutral or ionised depends on the position of the Fermi level as illustrated schematically in Fig. 5.10. A wealth of detailed information about the electronic states of point defects in these materials has been obtained by a variety of spectroscopic means and has been compiled, e.g., by SCHULZ [14].

Let us consider vacancies and self-interstitials $X \in (V, I)$ and suppose that both occur in various ionised states, which we denote by $j \in (0, 1\pm, 2\pm, \dots)$. The total concentration of the defect X at thermal equilibrium can be written as

$$C_X^{eq} = C_{X^0}^{eq} + C_{X^{1+}}^{eq} + C_{X^{1-}}^{eq} + C_{X^{2+}}^{eq} + C_{X^{2-}}^{eq} + \dots \quad (5.42)$$

Whereas the equilibrium concentration of uncharged defects depends only on temperature (and pressure), the concentration of charged defects is additionally influenced by the position of the Fermi level and hence by the doping level. If the Fermi level changes due to, e.g., *background doping* the concentration of charged defects will change as well.

The densities of electrons, n , and of holes, p , are tied to the intrinsic carrier density, n_i , via the law of mass action relation

$$np = n_i^2 \quad (5.43)$$

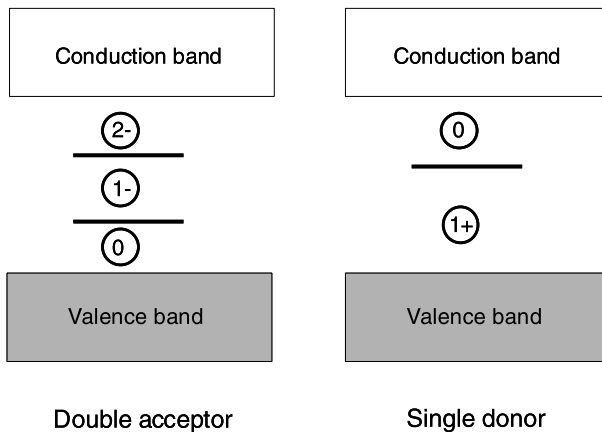


Fig. 5.10. Electronic structure of semiconductors, with a defect with double acceptor character (*left*) and donor character (*right*)

Then, Eq. (5.42) can be rewritten as

$$C_X^{eq} = C_{X^0}^{eq} + C_{X^{1+}}^{eq} (n_i) \frac{n_i}{n} + C_{X^{1-}}^{eq} (n_i) \frac{n}{n_i} + C_{X^{2+}}^{eq} (n_i) \left(\frac{n_i}{n} \right)^2 + C_{X^{2-}}^{eq} (n_i) \left(\frac{n}{n_i} \right)^2 + \dots, \quad (5.44)$$

where $C_{X^{j\pm}}^{eq}(n_i)$ denotes the equilibrium concentration under intrinsic conditions for defect X with charge state $j\pm$. From Eq. (5.44) it is obvious that n-doping will enhance (decrease) the equilibrium concentration of negatively (positively) charged defects. Correspondingly, p-doping will enhance (decrease) the equilibrium concentration positively (negatively) charged defects.

Furthermore, the ratio n/n_i varies with temperature because the intrinsic carrier density according to

$$n_i = \sqrt{N_{\text{eff}}^c N_{\text{eff}}^v} \exp\left(-\frac{E_g}{2k_B T}\right) \quad (5.45)$$

increases with increasing temperature. N_{eff}^c and N_{eff}^v denote the effective densities of states in the conduction and valence band, respectively. The values of n_i at different temperatures are determined mainly by the band gap energy E_g of the semiconductor. For a given background doping concentration the ratio n/n_i will be large at low temperatures and approaches unity at high temperatures. Then, the semiconductor reaches intrinsic conditions. The band gap energy is characteristic for a given semiconductor. It increases in the sequence Ge (0.67 eV), Si (1.14 eV), GaAs (1.43 eV). The intrinsic carrier density at a fixed temperature is highest for Ge and lowest for GaAs. Thus, doping effects on the concentration of charged defects are most prominent for GaAs and less pronounced for the elemental semiconductors.

Let us consider as an example a defect X which introduces a single X^{1-} and a double X^{2-} acceptor state with energy levels $E_{X^{1-}}$ and $E_{X^{2-}}$ above the valence band edge. Then, the ratios between charged and uncharged defect populations in thermal equilibrium are given by

$$\frac{C_{X^{1-}}^{eq}}{C_{X^0}^{eq}} = \frac{1}{g_{X^{1-}}} \exp\left(\frac{E_f - E_{X^{1-}}}{k_B T}\right),$$

$$\frac{C_{X^{2-}}^{eq}}{C_{X^0}^{eq}} = \frac{1}{g_{X^{2-}}} \exp\left(\frac{2E_f - E_{X^{2-}} - E_{X^{1-}}}{k_B T}\right), \quad (5.46)$$

where E_f denotes the position of the Fermi level. The degeneracy factors $g_{X^{1-}}$ and $g_{X^{2-}}$ take into account the spin degeneracy of the defect and the degeneracy of the valence band. The total concentration of point defects in thermal equilibrium for the present example is given by

$$C_X^{eq} = C_{X^0}^{eq} \left(1 + \frac{C_{X^{1-}}^{eq}}{C_{X^0}^{eq}} + \frac{C_{X^{2-}}^{eq}}{C_{X^0}^{eq}} \right). \quad (5.47)$$

Diffusion in semiconductors is affected by doping since defects in various charge states can act as diffusion-vehicles. Diffusion experiments are usually carried out at temperatures between the melting temperature T_m and about $0.6 T_m$. As the intrinsic carrier density increases with increasing temperature, doping effects in diffusion are more pronounced at the low temperature end of this interval. One can distinguish two types of doping effects:

- *Background doping* is due to a homogeneous distribution of donor or acceptor atoms, that are introduced during the process of crystal growing. Background doping is relevant for diffusion experiments, when at the diffusion temperature the carrier density exceeds the intrinsic density.
- *Self-doping* is relevant for diffusion experiments of donor or acceptor elements. If the in-diffused dopant concentration exceeds either the intrinsic carrier density or the available background doping, complex diffusion profiles can arise.

References

1. J.I. Frenkel, Z. Physik **35**, 652 (1926)
2. C. Wagner, W. Schottky, Z. Physik. Chem. B **11**, 163 (1931)
3. C.P. Flynn, *Point Defects and Diffusion*, Clarendon Press, Oxford, 1972
4. A.M. Stoneham, *Theory of Defects in Solids*, Clarendon Press, Oxford, 1975
5. F. Agullo-Lopez, C.R.A. Catlow, P. Townsend, *Point Defects in Materials*, Academic Press, London, 1988
6. H.J. Wollenberger, *Point Defects*, in: *Physical Metallurgy*, R.W. Cahn, P. Haasen (Eds.), North-Holland Publishing Company, 1983, p. 1139
7. L.W. Barr, A.B. Lidiard, *Defects in Ionic Crystals*, in: *Physical Chemistry – An Advanced Treatise*, Academic Press, New York, Vol. X, 1970
8. R.G. Fuller, *Ionic Conductivity including Self-diffusion*, in: *Point Defects in Solids*, J. M. Crawford Jr., L.M. Slifkin (Eds.), Plenum Press, 1972, p. 103
9. A. Seeger, D. Schumacher, W. Schilling, J. Diehl (Eds.), *Vacancies and Interstitials in Metals*, North-Holland Publishing Company, Amsterdam, 1970
10. N.L. Peterson, R.W. Siegel (Eds.), *Properties of Atomic Defects in Metals*, North-Holland Publishing Company, Amsterdam, 1978
11. C. Abromeit, H. Wollenberger (Eds.), *Vacancies and Interstitials in Metals and Alloys*; also: Materials Science Forum **15–18**, 1987
12. O. Kanert, J.-M. Spaeth (Eds.), *Defects in Insulating Materials*, World Scientific Publ. Comp., Ltd., Singapore, 1993
13. H. Ullmaier (Vol. Ed.), *Atomic Defects in Metals*, Landolt-Börnstein, New Series, Group III: Crystal and Solid State Physics, Vol. 25, Springer-Verlag, Berlin and Heidelberg, 1991
14. M. Schulz, Landolt-Börnstein, New Series, Group III: Crystal and Solid State Physics, Vol. 22: Semiconductors, Subvolume B: *Impurities and Defects in Group IV Elements and III-V Compounds*, M. Schulz (Ed.), Springer-Verlag, 1989

15. N.A. Stolwijk, Landolt-Börnstein, New Series, Group III: Crystal and Solid State Physics, Vol. 22: Semiconductors, Subvolume B: *Impurities and Defects in Group IV Elements and III-V Compounds*, M. Schulz (Ed.), Springer-Verlag, 1989, p. 439
16. N.A. Stolwijk, H. Bracht, Landolt-Börnstein, New Series, Group III: Condensed Matter, Vol. 41: Semiconductors, Subvolume A2: *Impurities and Defects in Group IV Elements, IV-IV and III-V Compounds*, M. Schulz (Ed.), Springer-Verlag, 2002, p. 382
17. H. Bracht, N.A. Stolwijk, Landolt-Börnstein, New Series, Group III: Condensed Matter, Vol. 41: Semiconductors, Subvolume A2: *Impurities and Defects in Group IV Elements, IV-IV and III-V Compounds*, M. Schulz (Ed.), Springer-Verlag, 2002, p. 77
18. F. Benière, *Diffusion in Alkali and Alkaline Earth Halides*, in: *Diffusion in Semiconductors and Non-metallic Solids*, Landolt-Börnstein, New Series, Group III: Condensed Matter, Vol. 33, Subvolume B1, D.L. Beke (Vol.Ed.). Springer-Verlag, 1999
19. G. Erdelyi, *Diffusion in Miscellaneous Ionic Materials*, in: *Diffusion in Semiconductors and Non-metallic Solids*, Landolt-Börnstein, New Series, Group III: Condensed Matter, Vol. 33, Subvolume B1, D.L. Beke (Vol.Ed.). Springer-Verlag, 1999
20. A. Seeger, H. Mehrer, *Analysis of Self-diffusion and Equilibrium Measurements*, in: *Vacancies and Interstitials in Metals*, A. Seeger, D. Schumacher, J. Diehl and W. Schilling (Eds.), North-Holland Publishing Company, Amsterdam, 1970, p. 1
21. R. Feder, A.S. Nowick, Phys. Rev. **109**, 1959 (1958)
22. R.O. Simmons, R.W. Balluffi, Phys. Rev. **117**, 52 (1960); Phys. Rev. **119**, 600 (1960); Phys. Rev. **129**, 1533 (1963); Phys. Rev. **125**, 862 (1962)
23. R.O. Simmons, R.W. Balluffi, Phys. Rev. **125**, 862 (1962)
24. A. Seeger, J. Phys. F. Metal Phys. **3**, 248 (1973)
25. R.O. Simmons, R.W. Balluffi, Phys. Rev. **117**, 52 (1960)
26. G. Bianchi, D. Mallejac, Ch. Janot, G. Champier, Compt. Rend. Acad. Science, Paris **263** 1404 (1966)
27. B. von Guerard, H. Peisl, R. Sizmann, Appl. Phys. **3**, 37 (1973)
28. H.-E. Schaefer, R. Gugelmeier, M. Schmolz, A. Seeger, J. Materials Science Forum **15–18**, 111 (1987)
29. M. Doyama, R.R. Hasiguti, Cryst. Lattice Defects **4**, 139 (1973)
30. P. Hautojärvi, Materials Science Forum **15–18**, 81 (1987)
31. H.-E. Schaefer, W. Stuck, F. Banhart, W. Bauer, Materials Science Forum **15–18**, 117 (1987)
32. W.M. Lomer, *Vacancies and other Point Defects in Metals and Alloys*, Institute of Metals, 1958
33. J. E. Dorn, J.B. Mitchell, Acta Metall. **14**, 71 (1966)
34. G. Berces, I. Kovacs, Philos. Mag. **15**, 883 (1983)
35. C. Tubandt, E. Lorenz, Z. Phys. Chem. **87**, 513, 543 (1914)
36. J. Maier, *Physical Chemistry of Ionic Solids – Ions and Electrons in Solids*, John Wiley & Sons, Ltd, 2004
37. A.R. Allnatt, A.B. Lidiard, *Atomic Transport in Solids*, Cambridge University Press, 1993
38. R. Friauf, Phys. Rev. **105**, 843 (1957)

39. R. Friauf, *J. Appl. Phys. Supp.* **33**, 494 (1962)
40. J.H. Westbrook, *Structural Intermetallics*, R. Dariola, J.J. Lewendowski, C.T. Liu, P.L. Martin, D.B. Miracle, M.V. Nathal (Eds.), Warrendale, PA, TMS, 1993
41. G. Sauthoff, *Intermetallics*, VCH Verlagsgesellschaft, Weinheim, 1995
42. Y.A. Chang, J.P. Neumann, *Progr. Solid State Chem.* **14**, 221 (1982)
43. H. Bakker, *Tracer Diffusion in Concentrated Alloys*, in: *Diffusion in Crystalline Solids*, G.E. Murch, A.S. Nowick (Eds.), Academic Press, Inc., 1984, p. 189
44. H.-E. Schaefer, K. Badura-Gergen, *Defect and Diffusion Forum* **143–147**, 193 (1997)
45. Th. Hehenkamp, *J. Phys. Chem. Solids* **55**, 907 (1994)
46. N.A. Stolwijk, M. van Gend, H. Bakker, *Philos. Mag. A* **42**, 783 (1980)
47. W. Frank, U. Gösele, H. Mehrer, A. Seeger, *Diffusion in Silicon and Germanium*, in: *Diffusion in Crystalline Solids*, G.E. Murch, A.S. Nowick (Eds.), Academic Press, Inc., 1984, p. 64
48. K. Girgis, *Structure of Intermetallic Compounds*, in: *Physical Metallurgy*, R.W. Cahn, P. Haasen (Eds.), North-Holland Physics Publishing, 1983, p. 219
49. M. Schulz (Vol.-Ed.), *Impurities and Defects in Group IV Elements, IV-IV and III-V Compounds*, Landolt-Börnstein, Group III, Vol. 41, Subvolume A2, Springer-Verlag, 2002
50. T.Y. Tan, U. Gösele, *Diffusion in Semiconductors*, in: *Diffusion in Condensed Matter – Methods, Materials, Models*, P. Heitjans, J. Kärger (Eds.), Springer-Verlag, 2005